

Mobility anisotropy of two-dimensional hole systems in (311)A GaAs/Al_xGa_{1-x}As heterojunctions

J. J. Heremans, M. B. Santos, K. Hirakawa, and M. Shayegan

Department of Electrical Engineering, Princeton University, Princeton, New Jersey 08544

(Received 22 September 1993; accepted for publication 8 April 1994)

We have measured the low-temperature mobility of high-quality two-dimensional hole systems confined at the (311)A GaAs/Al_xGa_{1-x}As interface. Variables were the thickness of the spacer layer separating the carriers from the Si dopants, and the carrier sheet density. A large anisotropy in mobility is found between the $[2\bar{3}3]$ and $[0\bar{1}\bar{1}]$ directions. While the high mobility $[2\bar{3}3]$ direction yields results analogous to the two-dimensional electron case, we conclude that transport along $[0\bar{1}\bar{1}]$ is almost entirely determined by anisotropic interface roughness scattering.

A significant improvement in two-dimensional hole system (2DHS) mobility was recently noted in remotely *p*-doped GaAs/Al_xGa_{1-x}As heterostructures obtained by molecular beam epitaxy (MBE) on the GaAs(311)A surface, where Si incorporates as an acceptor.¹⁻⁵ The hole transport mean free path in these 2DHSs reaches 10 μm, and ballistic hole behavior has been previously reported.^{5,6} While some work has dealt with the mobilities achievable in *p*-type Be-doped (100) samples,⁷ in the (311)A case still little is charted about either the growth on the GaAs (311)A surface, or about the hole transport properties in the resulting 2DHSs. Here we will present results on the latter. We find that the (311)A samples display a considerable anisotropy in the mobility; while scattering in the high mobility direction can be well understood as a straightforward extrapolation to heavier effective mass compared to two-dimensional electron systems (2DESs), the low mobility direction requires the introduction of anisotropic interface roughness scattering.

The samples were fabricated from a series of nearly identical MBE grown GaAs/Al_xGa_{1-x}As heterostructures. These consisted of a 1-μm-thick GaAs buffer layer, an undoped Al_{0.35}Ga_{0.65}As spacer layer of variable thickness (*s*), a narrow *p*-type Si-doped Al_{0.35}Ga_{0.65}As layer with doping density $2 \times 10^{18} \text{ cm}^{-3}$, and finally a sequence comprising another Si-doped layer intended to compensate for surface states. The thickness *s* separating the 2DHS from the Si dopant layer ranged from 250 to 1180 Å. As a rule, the 2DHSs at (311)A heterojunctions feature an anisotropy in the mobility μ ,^{2,5,6,8} the mobility along $[2\bar{3}3]$ can be up to 4 times higher than along $[0\bar{1}\bar{1}]$. In order to measure this transport anisotropy, we deep etched a double Hall bar pattern on all samples, using an H₂SO₄/H₂O₂/H₂O mesa etch after lithography. The perpendicular arms of the Hall bar were carefully aligned to the $[2\bar{3}3]$ and $[0\bar{1}\bar{1}]$ directions (inset of Fig. 1). Electrical contacts were achieved by alloying a near-eutectic In:Zn mixture in forming gas ambient. Finally, we deposited a Cr/Au front gate on some samples, allowing the hole sheet density *p* to be varied. All measurements were performed at 0.5 K.

The upper panel of Fig. 1 shows the density *p*, obtained from high field Hall effect measurements, versus the spacer width *s* for ungated samples. The monotonical decrease in *p* as *s* is increased has been well documented for 2DESs, and can be largely attributed to the decrease in electric field at the

heterointerface. In the lower panel we show the measured zero-field mobilities along $[2\bar{3}3]$ (henceforth designated by μ_H) and along $[0\bar{1}\bar{1}]$ (μ_L), as a function of *s*. Although the data of Fig. 1 were taken on samples from different wafers, it seems that the growth conditions were sufficiently reproducible to enable us to state the following observations.

Both μ_H and μ_L reach a pronounced maximum for *s* around 600 Å, corresponding to $p \approx 1 \times 10^{11} \text{ cm}^{-2}$. This behavior is similar to the 2DES case⁹ and results from the competing effects engendered by an increase in *s*. We consider the main scattering mechanisms to be remote ionized impurity scattering (from the intentionally doped Al_{0.35}Ga_{0.65}As layer), unintentional ionized impurity scattering (from residual impurities in both the GaAs channel and Al_{0.35}Ga_{0.65}As spacer), and interface roughness scattering at the heterointerface. These mechanisms separately lead to mobilities that we will denote by μ_{rm} , μ_{bk} , and μ_{ir} , respectively. With decreasing *s*, μ_{rm} decreases while μ_{bk} increases (following the increase in *p*). A larger *p* also means a higher electric field at the heterointerface, and thus enhanced interface roughness scattering and lower μ_{ir} . Combining the three together using Matthiessen's rule,¹⁰ the validity of which at sufficiently low temperatures we will assume throughout this work, the total mobility features the observed maximum. It is worth noting that the value of *s* at which the maxima in Fig. 1 occur lies very close to that found for *n*-type samples.⁹ Indeed, this optimal *s* ($\approx 600 \text{ Å}$) follows from the functional dependence of the different scattering mechanisms on *p*, rather than from their absolute values, and hence is rather insensitive to the effective mass of the carriers.

Although the hole dispersion displays some anisotropy, and hence the mass in the $[2\bar{3}3]$ and $[0\bar{1}\bar{1}]$ directions is not expected to be identical, the magnitude of the measured mobility ratios seems too substantial to be fully explained by this effect.^{3,6} We estimate the mass anisotropy to lead to a mobility ratio less than about 1.5 at $p \approx 2 \times 10^{11} \text{ cm}^{-2}$,⁶ far below the measured ratios. We believe this mobility anisotropy can be ascribed to anisotropic interface roughness scattering. In the case of 2DESs at GaAs/Al_xGa_{1-x}As (100) interfaces Tokura *et al.*¹¹ have observed a mobility anisotropy, and have correlated it to the anisotropy of the interface structure. For MBE-grown (311)A GaAs surfaces Noetzel *et al.*⁸ have reported the formation of periodic steps, with a period of 32 Å and a height of 10 Å, along the $[2\bar{3}3]$ orientation at

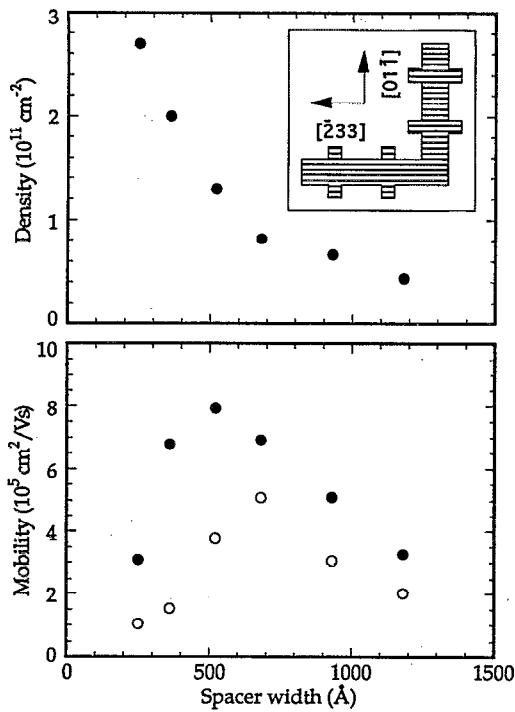


FIG. 1. Upper panel: the density p vs spacer width s (inset: double Hall bar with arms oriented along the $[233]$ and $[01\bar{1}]$ directions). Lower panel: μ_H (along $[233]$, filled circles) and μ_L (along $[01\bar{1}]$, open circles) vs s .

heterointerfaces. It seems reasonable therefore to invoke an additional scattering mechanism operative predominantly along the $[01\bar{1}]$ direction based on this interface morphology.

The wave vector associated with the periodicity of the steps, $2\pi/32 \text{ \AA}^{-1}$, is much larger than $2k_F$, where $k_F = (2\pi p)^{1/2}$ stands for the Fermi wave vector of the 2DHS, and hence the regular grating itself is not expected to lead to severely enhanced scattering. Yet, irregularities in this grating could result in spurious interface structures which we expect to be elongated along $[233]$. If these irregularities occur predominantly with wave vectors comparable to $2k_F$, enhanced large-angle scattering, to which the mobility is quite sensitive, would result. Thus, in this picture the mobility anisotropy is seen as a consequence of an anisotropic μ_{ir} .

We experimentally tested this conjecture. Since the deviation from regularity of the stepped interfaces may vary from sample to sample, we varied p in individual samples by means of a front gate. The density p follows the expected linear dependence on the front gate voltage V_g , with the slope $\partial p/\partial V_g$ matching the geometrical capacitance of the front-gate-2DHS system to within 5%. In Fig. 2 the experimental μ_H and μ_L are plotted vs p as varied by the front gate for two samples, with $s=520$ and 930 \AA in the left- and right-hand panel, respectively. The upgoing trend of μ_H vs p bears a close similarity to observations in 2DESs at the GaAs/ $\text{Al}_x\text{Ga}_{1-x}\text{As}$ (100) interface, and the lower overall μ_H values can be well accounted for by the heavier hole masses compared to the conduction band mass. In contrast, μ_L 's negative slope vs p is remarkable, and is consistent with μ_L being limited by the interface roughness scattering.

Before presenting a simple model for a semiquantitative

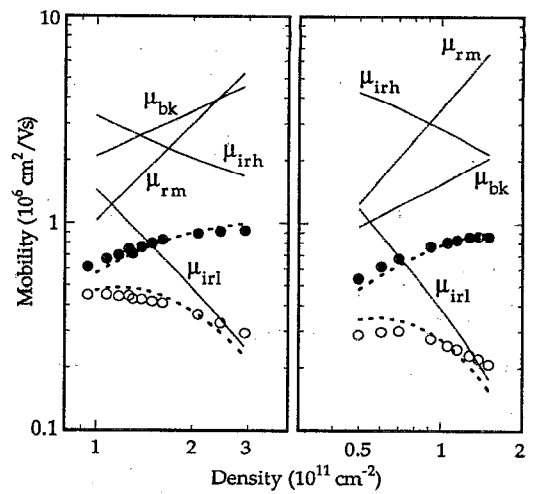


FIG. 2. Mobilities μ_H (filled circles) and μ_L (open circles) vs density p for two samples with different spacer widths s . The solid lines represent the calculated contributions from μ_{fm} (intentional dopant scattering), μ_{bk} (residual impurity scattering), μ_{irh} (interface roughness scattering along $[233]$), and μ_{ir} (along $[01\bar{1}]$). The resulting fits to μ_H and μ_L are shown as dashed lines. Left-hand panel: $s=520 \text{ \AA}$; $N_{bk}=1.4 \times 10^{14} \text{ cm}^{-3}$, $N_{fm}=3.0 \times 10^{11} \text{ cm}^{-2}$, $\Delta=2.4 \text{ \AA}$, $\Lambda=170 \text{ \AA}$, and $\epsilon=10$. Right-hand panel: $s=930 \text{ \AA}$; $N_{bk}=1.9 \times 10^{14} \text{ cm}^{-3}$, $N_{fm}=5.0 \times 10^{11} \text{ cm}^{-2}$, $\Delta=4.7 \text{ \AA}$, $\Lambda=250 \text{ \AA}$, and $\epsilon=70$.

understanding of the data of Fig. 2, we wish to point out the following results from measurements on our 2DHSs. In Fig. 2, both μ_H and μ_L follow a smooth dependence on p , without abrupt breaks, indicating that the number of occupied energy levels is not altered by increasing p . A Fourier transform of the Shubnikov-de Haas oscillations at low magnetic field (not shown) reveals that these levels consist of the two spin-split components of the lowest electrical subband. The spin degeneracy is lifted only at $\mathbf{k} \neq 0$ and results from the absence of inversion symmetry in the triangular wells.¹² Two carrier species with different effective masses (m_+ and m_-) are thus present. From the Fourier transform, and assuming parabolic bands, we find $m_-/m_+ \approx 0.6$. Cyclotron resonance measurements¹³ indicate $m_+ \approx 0.37m_0$ (where m_0 stands for the free electron mass) and hence we conclude $m_- \approx 0.23m_0$.

To understand the variation of μ_H and μ_L with p and to analyze the hole scattering mechanisms in our 2DHSs, we present here an approximate model including μ_{fm} , μ_{bk} , and μ_{ir} . We neglect the possibility of intersubband scattering between the two hole bands.¹⁴ We take the effective mass values m_+ and m_- to be 0.37 and $0.23 m_0$, respectively. Screening is included in the long wavelength limit and a Fang-Howard wave function is used, neglecting the penetration into the spacer layer.¹⁵ The residual impurity concentration in both the GaAs channel and $\text{Al}_{0.35}\text{Ga}_{0.65}\text{As}$ spacer appearing in μ_{bk} , are assumed identical. The depletion charge in the GaAs channel was taken to be constant at $5 \times 10^{10} \text{ cm}^{-2}$. The calculation of μ_{bk} follows that outlined in Ref. 16. As in Refs. 17 and 11, the interface roughness is characterized by a step height Δ of the irregularities and a lateral correlation length Λ . We added to μ_{ir} the effect in a triangu-

lar well of a gate voltage induced variable electric field. Anisotropic roughness scattering is treated in Ref. 11, whose authors assume a distribution of elliptical scattering islands. The length of the islands is taken a factor $(1+\epsilon)^{1/2}$ larger than their width, where the eccentricity ϵ is handled as a fitting parameter. Solving the Boltzmann equation to linear order yields, in our case, μ_{ir} (along $[01\bar{1}]$) and μ_{ih} (along $[\bar{2}33]$), respectively.

Under these assumptions, we have simultaneously fitted both the experimental μ_H and μ_L . The fitting parameters were, for μ_{bk} the residual impurity concentration N_{bk} , for μ_{rm} the density N_{rm} of the remote ionized Si dopants, and for μ_{ir} the height Δ of the interface irregularities, the correlation length Λ , and the eccentricity ϵ . Figure 2 shows the individual contributions of μ_{rm} , μ_{bk} , and the two μ_{ir} (solid lines) as well as the resulting theoretical μ_H and μ_L for the chosen values of the parameters (dashed lines). Although we feel the behavior of μ_H and μ_L has been well reproduced and the fit is quite close for reasonable parameter values, no quantitative significance should be attached to the numbers obtained for N_{bk} , N_{rm} , Λ , Δ , and ϵ .

Some broad conclusions can be safely inferred however. N_{bk} and N_{rm} are similar in both samples; N_{rm} of the order of several times 10^{11} cm^{-2} compares well to the Si sheet density of nominally $9 \times 10^{11} \text{ cm}^{-2}$ in the narrow doped layer, and N_{bk} in the low 10^{14} cm^{-3} can be expected for a clean MBE system. Reminiscent of 2DESSs, μ_{rm} varies with s and p as $(s^3)(p^{3/2})$, while μ_{bk} follows a less strong p dependence. As a comparison of the left- and right-hand panels shows, μ_{rm} plays a more significant role in the sample with the smaller $s=520 \text{ \AA}$. Yet, overall both Coulomb scattering mechanisms (μ_{rm} and μ_{bk}) tend to influence the mobility only at lower p , while μ_{ih} becomes the limiting mechanism for μ_H at higher p . In contrast, μ_L is almost completely determined by μ_{ir} . The same trend can be spotted in Fig. 1 (despite the scatter due to variable sample parameters), where the mobility anisotropy grows more extreme at higher p . Finally, we note that in the fits of Fig. 2, Δ for both samples is close to one monolayer, while the more extreme anisotropy of the sample with $s=930 \text{ \AA}$ necessitates a larger $\epsilon=70$, corresponding to islands having a length to width ratio of 8 as compared to 3 in the other sample.

In summary, we have presented a study of the mobilities of 2DHSs at GaAs/Al_xGa_{1-x}As heterostructures obtained by MBE on the GaAs (311)A surface. The behavior of μ_H , along $[\bar{2}33]$, vs p in samples of different spacer width, or in

individual samples where p was varied via a front gate, mimics previous observations in 2DESSs, the differences arising mainly from the heavier hole masses. In the $[01\bar{1}]$ direction however, μ_L stays much below the expected values and decreases with increasing p . From a simplified model we infer that interface roughness scattering, while playing a minor role in μ_H , entirely dominates μ_L , and is responsible for the measured mobility anisotropy.

We thank S. R. Parihar for helpful discussions. This work was supported by the National Science Foundation, the Army Research Office, and the IBM Corporation. The authors are affiliated with the Advanced Technology Center for Photonics and Optoelectronic Materials established at Princeton University by the State of New Jersey.

- ¹W. I. Wang, E. E. Mendez, T. S. Kuan, and L. Esaki, *Appl. Phys. Lett.* **47**, 826 (1985).
- ²A. G. Davies, J. E. F. Frost, D. A. Ritchie, D. C. Peacock, R. Newbury, E. H. Linfield, M. Pepper, and G. A. C. Jones, *J. Cryst. Growth* **111**, 318 (1991).
- ³R. K. Hayden, E. C. Valadares, M. Henini, L. Eaves, D. K. Maude, and J. C. Portal, *Phys. Rev. B* **46**, 15586 (1992); E. C. Valadares, *ibid.* **46**, 3935 (1992).
- ⁴M. B. Santos, Y. W. Suen, M. Shayegan, Y. P. Li, L. W. Engel, and D. C. Tsui, *Phys. Rev. Lett.* **68**, 1188 (1992).
- ⁵J. J. Heremans, M. B. Santos, and M. Shayegan, *Appl. Phys. Lett.* **61**, 1652 (1992).
- ⁶J. J. Heremans, M. B. Santos, and M. Shayegan, *Surf. Sci.* **305**, 348 (1994).
- ⁷H. L. Stormer, A. C. Gossard, W. Wiegmann, R. Blondel, and K. Baldwin, *Appl. Phys. Lett.* **44**, 139 (1984); W. I. Wang, E. E. Mendez, and F. Stern, *ibid.* **45**, 639 (1985).
- ⁸R. Noetzel, N. N. Ledentsov, L. Daeweritz, K. Ploog, and M. Hohenstein, *Phys. Rev. B* **45**, 3507 (1992).
- ⁹F. Stern, *Appl. Phys. Lett.* **43**, 974 (1983); J. J. Harris, C. T. Foxon, K. W. J. Barnham, D. E. Lacklison, J. Hewett, and C. White, *J. Appl. Phys.* **61**, 1219 (1987).
- ¹⁰F. Stern, *Phys. Rev. Lett.* **44**, 1469 (1980).
- ¹¹Y. Tokura, T. Saku, S. Tarucha, and Y. Horikoshi, *Phys. Rev. B* **46**, 15558 (1992).
- ¹²J. P. Eisenstein, H. L. Stormer, V. Narayanamurti, A. C. Gossard, and W. Wiegmann, *Phys. Rev. Lett.* **53**, 2579 (1984).
- ¹³K. Hirakawa, Y. Zhao, M. B. Santos, M. Shayegan, and D. C. Tsui, *Phys. Rev. B* **47**, 4076 (1993).
- ¹⁴The same approximation was used by W. Walukiewicz, *Phys. Rev. B* **31**, 5557 (1985).
- ¹⁵F. Stern, *Phys. Rev. Lett.* **18**, 546 (1967); G. Bastard, *Wave Mechanics Applied to Semiconductor Heterojunctions* (Halsted, New York, 1988); T. Ando, A. B. Fowler, and F. Stern, *Rev. Mod. Phys.* **54**, 437 (1982).
- ¹⁶A. Gold, *Appl. Phys. Lett.* **54**, 2100 (1989).
- ¹⁷H. Sakaki, T. Noda, K. Hirakawa, M. Tanaka, and T. Matsusue, *Appl. Phys. Lett.* **51**, 1934 (1987); T. Ando, *J. Phys. Soc. Jpn.* **51**, 3900 (1982); T. Noda, M. Tanaka, and H. Sakaki, *J. Cryst. Growth* **95**, 60 (1989).